Immunophilin-like TWISTED DWARF1 modulates auxin efflux activities of Arabidopsis p-glycoproteins

THE JOURNAL OF BIOLOGICAL CHEMISTRY VOL. 281, NO. 41, pp. 30603–30612, October 13, 2006

Immunophilin-like TWISTED DWARF1 Modulates Auxin Efflux Activities of *Arabidopsis* P-glycoproteins*[S]

Received for publication, May 12, 2006, and in revised form, July 18, 2006 Published, JBC Papers in Press, August 3, 2006, DOI 10.1074/jbc.M604604200

Rodolphe Bouchard[‡], Aurélien Bailly[‡], Joshua J. Blakeslee[§], Sophie C. Oehring[‡], Vincent Vincenzetti[‡], Ok Ran Lee[§1], Ivan Paponov[¶], Klaus Palme[¶], Stefano Mancuso[‖], Angus S. Murphy[§], Burkhard Schulz[§], and Markus Geisler[‡2]

From the [‡]Zurich-Basel Plant Science Center, University of Zurich, Institute of Plant Biology, and Molecular Plant Physiology, CH-8008 Zurich, Switzerland, the [§]Department of Horticulture and Landscape Architecture, Purdue University, West Lafayette, Indiana 47907, the [¶]Institut für Biologie II, Universität Freiburg, D-79104 Freiburg, Germany, and the [‖]Department of Horticulture, University of Firenze, I-50019 Sesto Fiorentino, Italy

The immunophilin-like protein TWISTED DWARF1 (TWD1/FKBP42) has been shown to physically interact with the multidrug resistance/P-glycoprotein (PGP) ATP-binding cassette transporters PGP1 and PGP19 (MDR1). Overlapping phenotypes of *pgp1*/*pgp19* and *twd1* mutant plants suggested a positive regulatory role of TWD1 in PGP-mediated export of the plant hormone auxin, which controls plant development. Here, we provide evidence at the cellular and plant levels that TWD1 controls PGP-mediated auxin transport. *twd1* and *pgp1*/*pgp19* cells showed greatly reduced export of the native auxin indole-3-acetic acid (IAA). Constitutive overexpression of PGP1 and PGP19, but not TWD1, enhanced auxin export. Coexpression of TWD1 and PGP1 in yeast and mammalian cells verified the specificity of the regulatory effect. Employing an IAA-specific microelectrode demonstrated that IAA influx in the root elongation zone was perturbed and apically shifted in *pgp1*/*pgp19* and *twd1* roots. Mature roots of *pgp1*/*pgp19* and *twd1* plants revealed elevated levels of free IAA, which seemed to account for agravitropic root behavior. Our data suggest a novel mode of PGP regulation via FK506-binding protein-like immunophilins, implicating possible alternative strategies to overcome multidrug resistance.

The plant signaling molecule auxin (indole-3-acetic acid (IAA))[3] plays a critical role in plant growth and development (1, 2, 6). Moreover, IAA has been shown to have potential value as a photoactivable cytotoxin with applications in cancer therapy (7). Although auxin signaling shares some similarities with mammalian neurotransmitter signaling (3, 49), auxin is generally classified as a phytohormone because of its transport from sites of synthesis to loci of activity. Auxin transport is polar from the shoot apex to the root apex and in reverse to the root-hypocotyl junction in a cell-to-cell manner (4, 6). Polar auxin transport appears to provide essential directional and positional information for developmental and physiological processes (5). A chemiosmotic model of auxin transport (8, 9) was supported by the identification and characterization of candidate proteins for auxin influx (AUX1/LAX family) and efflux (PIN family) (reviewed in Refs. 2 and 4). Members of both families are essential components of auxin influx and efflux complexes, and most strikingly, the major proteins of both families (AUX1 and PIN1) reveal polar expression patterns that are congruent with known routes of auxin movement (6). Evidence has been provided for a model in which multiple PIN proteins interact to create an auxin reflux loop (5), and it has been shown recently that some members of the PIN family are rate-limiting factors in cellular auxin efflux (10).

Recently, members of the large plant multidrug resistance (MDR)/P-glycoprotein (PGP)/ABCB family (hereafter referred to as PGP) have been shown to function in auxin transport (4, 11–13). Mammalian members of this superfamily of ATP-binding cassette (ABC) transporters are widely studied because they catalyze ATP-dependent export of planar anionic chemotherapeutic agents (14). Loss-of-function mutations in *PGP1* and *PGP19* (*MDR1*) result in reduced auxin transport in intact tissues and impaired growth in *Arabidopsis* (15–18), maize (*Zea mays pgp1*/*brachytic2*), and sorghum (*Sorghum bicolor pgp1*/*dwarf3*) (19). Interestingly, the dwarf phenotype of *pgp1*/*pgp19* double mutants is more severe than those of the single knockouts, suggesting separate but overlapping functions (16, 18). PGP1 has been shown to catalyze the primary active transport of native and synthetic auxins using plant and heterologous transport systems. PGP1 activity is inhibited by auxin efflux inhibitors such as *N*-1-naphthylphthalamic acid (NPA) and flavonols as well as anticancer drugs such as verapamil and cyclosporin A (17). Consistent with predictions from chemiosmotic models of sites requiring additional direct auxin efflux (4), PGP1 exhibits non-polar plasma membrane localization in small meristematic cells of the root and shoot apices and polar (mainly basal) expression in expanded cells of the elongation zone and above. Two recent studies showed that a related protein (PGP4) functions in root and root hair development and

* The costs of publication of this article were defrayed in part by the payment of page charges. This article must therefore be hereby marked "*advertisement*" in accordance with 18 U.S.C. Section 1734 solely to indicate this fact.
[S] The on-line version of this article (available at http://www.jbc.org) contains supplemental Figs. 1–6.
[1] Present address: Department of Biology Chungnam National University, Daejeon 305–764, Korea.
[2] To whom correspondence should be addressed: Inst. of Plant Biology, University of Zurich, Zolliker Strasse 107, CH-8008 Zurich, Switzerland. Tel.: 41-1-634-8276; Fax: 41-1-634-8204; E-mail: markus.geisler@botinst.unizh.ch.
[3] The abbreviations used are: IAA, indole-3-acetic acid; MDR, multidrug resistance; PGP, P-glycoprotein; ABC, ATP-binding cassette; NPA, *N*-1-naphthylphthalamic acid; FKBP, FK506-binding protein; MRP, MDR-associated protein; GFP, green fluorescent protein; GC-MS, gas chromatography-mass spectrometry; RT, reverse transcription; YFP, yellow fluorescent protein; CFP, cyan fluorescent protein; HA, hemagglutinin; NAA, naphthylacetic acid.

that it catalyzes substantial auxin influx (20, 21), suggesting that PGP1 and PGP4 might function cooperatively in auxin movement (13, 20).

Plant PGPs seem to function as central catalytic elements of multiprotein auxin transport complexes (4, 13, 16, 22). The C terminus of PGP1 has been identified in a yeast two-hybrid screen using the soluble portion of the putative glycosylphosphatidylinositol-anchored immunophilin-like protein TWISTED DWARF1 (TWD1/FKBP42) as bait (16). Moreover, several PGPs (including PGP1, PGP19, and PGP4) have been co-purified with TWD1 from high affinity NPA-binding complexes with other proteins known to be involved in protein trafficking and cycling (22, 16). *twd1* plants, which are allelic to *ultracurvata2* (*ucu2*) (23), show a drastic pleiotropic auxin-related phenotype that includes dwarfism, epinastically growing leaves, and disorientation of organ growth at both the epidermal and whole plant levels. Interestingly, *twd1* plants resemble those of *pgp1*/*pgp19* double mutants, and PGP1/PGP19-TWD1 interaction can be verified by a broad array of methods (16). Similar mutant phenotypes, together with reduced auxin transport in intact hypocotyls, suggested a regulatory role for PGP1 and PGP19 in auxin transport (13, 16, 24).

TWD1 belongs to the FK506-binding protein (FKBP)-type subfamily of immunophilins, which are ubiquitous proteins known to mediate immunosuppression in mammals (24, 28, 36). Based on drastic phenotypes of knock-out mutants and transgenic plants with altered gene expression levels, multidomain FKBPs such as PASTICCINO1 (FKBP52/PAS1) and wheat FKBP77 (25–27) have been found to be key players in plant development (28). TWD1, which also belongs to the multidomain FKBP family, is distinguished by its unique C-terminal membrane anchor, which localizes the protein to both the plasma (16) and vacuolar (29) membranes. In the latter, TWD1 functionally interacts with the C termini of MDR-associated protein (MRP)-like ABC transporters MRP1 and MRP2 (30). Interestingly, both pairs of ABC transporters interact with independent domains of TWD1. PGP1 and PGP19 interact with the *cis*,*trans*-peptidylprolyl isomerase-like domain, and MRP1 and MRP2 interact with the tetratricopeptide repeat domain. This difference in binding to TWD1 domains might specify functional diversity of the interactions.

In both cases, regulatory roles of TWD1 in individual ABC transporter pairs have been suggested (16, 30), but the final molecular proof is still lacking. Mammalian FKBPs are known to bind and modulate calcium release channels (31, 44). Furthermore, FKBP12 has been shown to regulate murine MDR3 activity, but attempts to demonstrate interaction have been thus far unsuccessful (33). Interestingly, FKBP12-dependent regulation of MDR3-mediated drug resistance does not require *cis*,*trans*-peptidylprolyl isomerase activity (31, 34). Consistent with these observations, the PGP-interacting *cis*,*trans*-peptidylprolyl isomerase-like domain of TWD1 has been shown to lack any isomerase activity and not to bind FK506 (29, 63). Here, we provide several lines of evidence that TWD1 functions as a positive regulator of PGP1-mediated auxin transport, suggesting a novel mode of PGP regulation via FKBP-type immunophilins.

EXPERIMENTAL PROCEDURES

Plant Growth Conditions—Arabidopsis thaliana plants were grown as described previously (16). For quantification of gravitropism, wild-type and *pgp1* (At2g36910), *pgp19* (At3g28860), *pgp1*/*pgp19*, and *twd1* (At3g21640) mutant seeds (all ecotype Wassilewskija) were surface-sterilized and grown on half-strength Murashige and Skoog medium and 0.7% Phytagar (Invitrogen, Paisley, UK) under continuous light conditions as described (61). Each gravistimulated root was assigned to one of twelve 30° sectors in the circular histograms; the length of each bar represents the percentage of seedlings showing the same direction of root growth. The number of seedlings for each genotype was between 72 and 96.

Analysis of IAA Contents and Responses—A. thaliana wild-type, *pgp1*, *pgp19*, *pgp1*/*pgp19*, and *twd1* mutant plants (all ecotype Wassilewskija) expressing the maximal auxin-inducible reporter Pro_{DR5}-green fluorescent protein (GFP) construct were generated by *Agrobacterium*-mediated transformations using the *DR5-GFPm* construct (38). Homozygous T3 was used for all experiments described. Seedlings were grown vertically for 5 days as described above, stained with 10 μM propidium iodide before microscopy, and analyzed by differential interference contrast (Leica DM R microscope equipped with a Leica DC300 F charge-coupled device). For histological signal localization, both images were electronically merged and further processed with Photoshop 7.0. (Adobe Systems Inc., Mountain View, CA).

For endogenous free auxin quantification, shoot and root segments of 30–50 seedlings were collected and pooled. The samples were extracted with MeOH and analyzed by gas chromatography-mass spectrometry (GC-MS). Calculation of isotopic dilution factors was based on the addition of 100 pmol of [^{2}H]IAA to each sample. In some cases, roots of 40 seedlings were manually divided into root segments (see Fig. 4*C*) and analyzed as described above. The data are presented the means of three independent lots of 30–50 seedlings each.

Expression and Localization Analysis—Immunolocalization in roots was performed as described (60). Labeling was performed with rabbit anti-PIN1 and guinea pig anti-PIN2 antibodies at 1:500 and 1:400 dilutions, respectively. Alexa Fluor 488-conjugated goat anti-rabbit and anti-guinea pig secondary antibodies were used at 1:400 dilution. During the immunolocalization procedures, solutions were changed using a pipetting robot (InsituPro, Intavis Bioanalytical Instruments AG). Plasma membranes and microsomal fractions were separated by aqueous two-phase partitioning or continuous sucrose gradient centrifugation and immunoprobed as described (16).

Transcript Detection by Reverse Transcription (RT)-PCR—Semiquantitative RT-PCR was performed as described (51). Transcripts specific for *PGP1* (At2g36910),*TWD1* (At3g21640), and 40 S ribosomal protein *S16* (At2g09990) were detected by conventional PCR for 25 and 30 cycles at an annealing temperature of 52 °C. The intron-spanning PCR primers used were as follows: S16, 5′-ggcgactcaaccagctactga (sense) and 5′-cggtaactctttggtaacga (antisense); PGP1, 5′-gtccctcaagagccgtgcttg (sense) and 5′-ccatcatcgatgacagcgatc (antisense); TWD1, 5′-ccatagcatacatgggggacg (sense) and 5′-tctgtggcgtcgaaagatacg (antisense). Equal volumes of

PCR products were separated on 2.5% agarose gels. Negative controls in the absence of enzyme in the RT reaction yielded no products.

Protoplast Efflux Experiments—Intact *Arabidopsis* mesophyll protoplasts were prepared from the rosette leaves of plants grown on soil under white light (100 μmol m^{-2} s^{-1}, 8-h light/16-h dark cycle, 22 °C), and auxin efflux experiments were performed as described (17). Briefly, intact protoplasts were isolated as described (16) and loaded by incubation with 1 μl/ml [^{3}H]IAA (specific activity of 20 Ci/mmol; American Radiolabeled Chemicals, Inc., St. Louis, MO) on ice. External radioactivity was removed by Percoll gradient centrifugation (17). Efflux was started by incubation at 25 °C and halted by silicon oil centrifugation. Effluxed radioactivity was determined by scintillation counting of the aqueous phases and is presented as relative efflux of the initial efflux (efflux prior to incubation), which was set to zero. Protoplast volumes, surfaces, and vacuolar pH were determined as described (17).

Yeast Assays—cDNAs from *Arabidopsis* TWD1 (At3g21640), FKBP12 (At1g58450), and ROF1 (At3g25230) were cloned into the BamHI and SalI sites of the copper-inducible yeast shuttle vector pRS314CUP (52). pNEV, pNEV-PGP1 (17), pRS314CUP, pRS314CUP-FKBP12, and pRS314CUP-ROF1 were introduced into *Saccharomyces cerevisiae* strains JK93dα (33) SMY87-4 (53), PJ69-4a (54), and *yap1-1* (40), and single colonies were grown in synthetic minimal medium without uracil and tryptophan and supplemented with 2% glucose and 100 μM $CuCl_2$. For detoxification assays, transformants grown in the same medium to $A_{600} \sim 0.8$ were washed and diluted to $A_{600} = 1.0$ in water. Cells were 10-fold diluted five times, and each 5 μl were spotted on minimal medium plates supplemented with 10 μM IAA or 750 μM 5-fluoroindole. Growth at 30 °C was assessed after 3–5 days. Assays were performed with three independent transformants.

IAA transport experiments were performed as described (17). For loading experiments (see Fig. 6, *C* and *D*; and supplemental Fig. 6*A*), cells were grown to $A_{600} = 1.0$, washed, and incubated at 30 °C with 1 μl/ml 5-[^{3}H]IAA (specific activity of 20 Ci/mmol; American Radiolabeled Chemicals, Inc.) in synthetic minimal medium (pH 4.5). Aliquots of 0.5 ml were taken after incubation at 30 °C. IAA retention is expressed as relative loading of the initial loading ($t = 2.5$ min), which was set to zero. For efflux experiments (see Fig. 6*B*), cells were loaded for 10 min on ice, washed twice with cold water, and resuspended in 15 ml of synthetic minimal medium (pH 4.5). Aliquots of 0.5 ml were taken after incubation at 30 °C. IAA retention is expressed as relative loading of the initial (maximal) loading ($t = 0$ min), which was set to 100%.

PGP1 and TWD1 Expression in Yeast and Immunolocalization—Yellow fluorescent protein (YFP) and cyan fluorescent protein (CFP) were amplified by PCR from plasmids pEYFP and pECFP (Clontech) inserted in-frame into AscI sites generated in the coding regions of pNEV-PGP1 (bp 2,674) and pRS314CUP-TWD1 (bp 64) using the QuikChange XL site-directed mutagenesis kit (Stratagene, La Jolla, CA). YFP and CFP were inserted into the cytoplasmic loop between transmembrane domains 10 and 11 of PGP1 and into the very N terminus of TWD1. Cells coexpressing PGP1-YFP and TWD1-CFP were incubated in mounting medium containing 4′,6-diamidino-2-phenylindole, and immunofluorescence analysis was performed using a Leica DM IRE2 confocal laser scanning microscope equipped with argon (488 nm) and UV (410 nm) lasers. Fluorescence and differential interference contrast images were processed using Photoshop 7.0. Vector controls showed no detectable fluorescence.

Yeast cells coexpressing PGP1 and TWD1 were grown to mid-log phase, and microsomes were separated via continuous sucrose gradient centrifugation (30). Plasma membrane fractions were subjected to 7.5% PAGE, and Western blots were immunoprobed using anti-PGP1 (58) and anti-TWD1 (16) antibodies.

HeLa Cell Assays—Radiolabeled substrate accumulation assays after transient coexpression of PGP1 (At2g36910) and TWD1 (At3g21640) at a 1:0.5 ratio were performed as described (17). Net efflux (the amount of auxin retained by cells transformed with empty vector minus the amount of auxin retained by cells transformed with PGP19) is expressed as disintegrations/min/500,000 cells. The average empty control vector value was 2852 disintegrations/min/500,000 cells.

In all cases, expression and localization of *PGP19* was confirmed by RT-PCR and Western blotting using standard protocols for the system (37, 55). Cell viability after treatment was confirmed visually and via cell counting.

Recording Root Apex Auxin Fluxes Using an IAA-specific Microelectrode—A platinum microelectrode (35) was used to monitor IAA fluxes in *Arabidopsis* roots as described (20). For measurements, plants were grown in hydroponic cultures and used 5 days after germination. Differential current from an IAA-selective microelectrode placed 2 μm from the root surface was recorded in a self-referencing mode. The sensor was vibrated between two positions 10 μm distant at a rate of 0.1 Hz.

Data Analysis—Data were analyzed using Prism 4.0b (GraphPad Software, San Diego, CA), and statistical analysis was performed using SPSS 11.0 (SPSS, Inc., Chicago, IL).

RESULTS

Cellular and Polar Transport of IAA Is Reduced in twd1 and pgp1/pgp19 Mutants, Indicating a Regulatory Role for TWD1—Recently, interactions between TWD1 and the MDR/PGP-type transporter PGP1 and its closest homolog, PGP19, were demonstrated (16). Indirect evidence suggests that TWD1 functions in part by regulating the overlapping auxin transport activities of PGP1 and PGP19 (13, 16, 17).

To demonstrate the physiological impact of TWD1 interaction, we measured PGP-mediated cellular efflux of radiolabeled auxin (IAA) in isolated leaf mesophyll protoplasts using silicon oil centrifugation (17). Protoplasts from *twd1* plants showed greatly reduced IAA efflux (48%) compared with those from wild-type plants (100%) (Fig. 1*A*). This reduction of efflux in *twd1* protoplasts was slightly (but not significantly) less than that observed in *pgp1*/*pgp19* protoplasts (49%) (17). These measurements correlate well with auxin transport rates found in intact tissues (16). The presence of PGP1, PGP19, and TWD1 in the assayed cells was verified both by RT-PCR in wild-type plants (Fig. 1*A*) and by Western analysis (Fig. 1, *B* and C). The

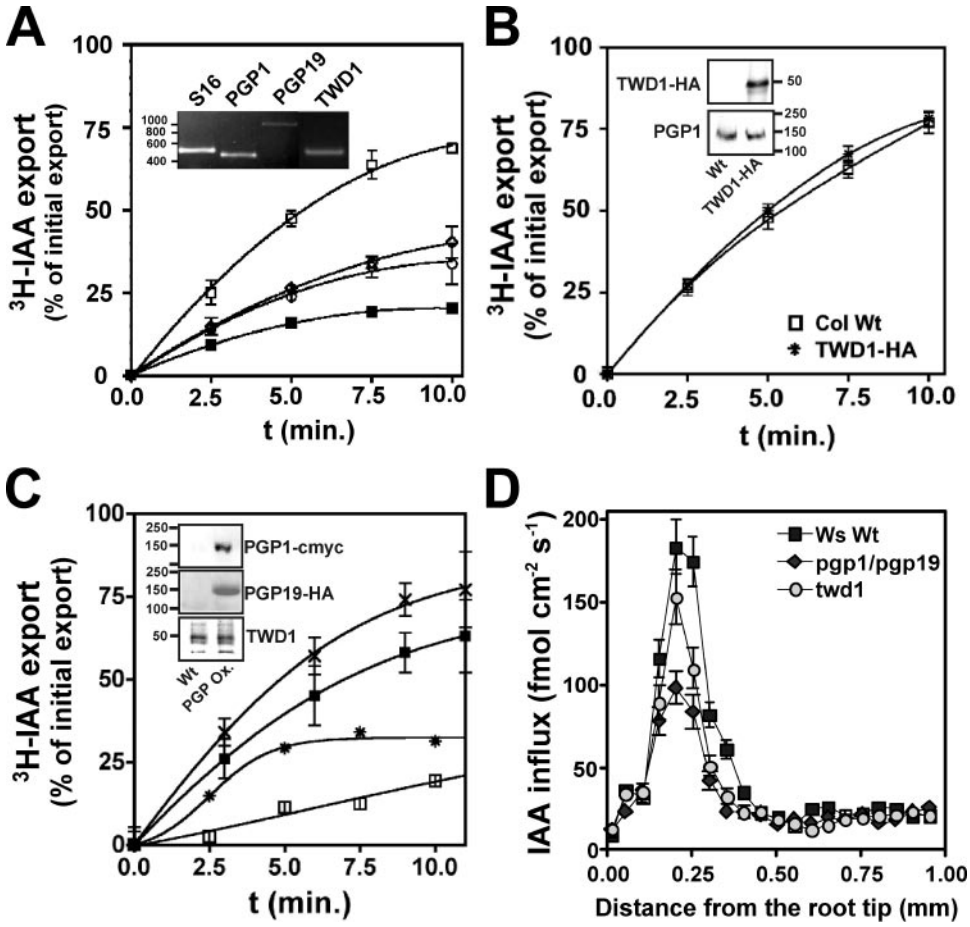

FIGURE 1. **Cellular IAA export is reduced in *twd1*, but is not affected by overexpression of TWD1.** *A*, cellular [^{3}H]IAA export in wild-type mesophyll protoplasts (ecotype Wassilewskija; □) was reduced to a similar extent in *twd1* (○) and *pgp1*/*pgp19* (◇) plants. We used de-energized (dark-treated) plant material (■) as a negative control. The presence of PGP1, PGP19, and TWD1 in wild-type protoplasts was verified by semiquantitative RT-PCR (*inset*). Efflux is presented as relative export of the initial export. Data are the means ± S.D. of three to five individual experiments ($n = 4$). *B*, constitutive overexpression of TWD1 did not alter [^{3}H]IAA export, suggesting a regulatory role of TWD1. Overexpression of TWD1-HA in protoplasts was verified by Western blot analysis using anti-HA antibody (16); overexpression of TWD1 did not alter expression of PGP1 or PGP19 (*inset*) as shown using anti-PGP1 antibody, which does not differentiate between PGP1 and PGP19 (16). *C*, constitutive overexpression of PGP1-c-Myc (*) and PGP19 (×) enhanced [^{3}H]IAA export compared with their corresponding wild-type (*Wt*) ecotypes, RLD (□) and Columbia (*Col*; ■), respectively. Overexpression (*Ox.*) of PGP1 and PGP19 in protoplasts was verified by Western blot analysis using anti-c-Myc and anti-HA antibodies. Overexpression of PGPs did not alter expression of TWD1 (*inset*) shown for PGP1. *D*, IAA influx was reduced in the transition zone of *pgp1*/*pgp19* and *twd1* roots. Shown is the IAA influx profile along single roots of wild-type, *pgp1*/*pgp19*, and *twd1* plants. Positive fluxes represent a net IAA influx. Data shown were collected continuously over a 10-min period and are the means of eight replicates; *error bars* represent S.E. *Ws*, Wassilewskija.

impact of interfering factors such as vacuolar trapping of IAA and reduced export capacities due to alterations in vacuolar pH (56) or in protoplast surfaces could be excluded (supplemental Fig. 1).

To further investigate the regulatory role of TWD1, we measured IAA efflux in protoplasts generated from *twd1* plants that were fully complemented by a $Pro_{CaMV35S}$-TWD1-hemagglutinin (HA) construct (16). Overexpression of TWD1-HA was verified by Western blotting and did not alter PGP1 or PGP19 expression (Fig. 1*B*, *inset*). Interestingly, IAA efflux in TWD1-overexpressor protoplasts was not significantly different from that in wild-type protoplasts (Fig. 1*B*), indicating that it is unlikely that TWD1 transports auxin directly. In contrast, constitutive up-regulation of PGP1 or PGP19 greatly enhanced IAA export compared with their corresponding wild-type ecotypes. Interestingly, *Arabidopsis* ecotypes RLD and Columbia seem to have ecotype-specific differences in auxin efflux capacity (Fig. 1*C*), consistent with previously documented whole plant ecotype-specific differences in auxin transport (32). The reduced increase in IAA efflux stimulated by PGP19 overexpression (122% of the wild-type level (100%)) compared with PGP1 overexpression (130% of the wild-type level) does not reflect the transport capacities of the individual proteins, but is instead the result of differences in expression levels as shown by RT-PCR (relative expression level compared with the wild-type level: PGP1, 8.0 ± 2.2; and PGP19, 3.0 ± 0.6).

To verify these data at the whole plant level, a novel self-referencing IAA-specific microelectrode was used to obtain noninvasive and continuous recordings of auxin fluxes in intact root apices (35). IAA influxes in *Arabidopsis* are characterized by a distinct peak at 0.2–0.3 mm from the root tip in the so-called root transition or distal elongation zone of the root apex (20), consistent with the current auxin "reflux" model describing auxin transport streams in roots (5). In wild-type roots, the transition zone auxin peak averaged 184.2 ± 16.5 fmol cm^{-2} s^{-1}, whereas in *twd1* roots, the maximal influx in the root transition zone was significantly reduced, averaging 153.6 ± 16 fmol cm^{-2} s^{-1}. (Fig. 1*D*). The influx in *pgp1*/*pgp19* roots was more severely reduced (98.5 ± 10.2 fmol cm^{-2} s^{-1}) (Fig. 1*D*). Interestingly, the IAA peak was less reduced in *twd1* roots (Fig. 1*D*) than in *pgp1* and *pgp19* single mutant roots (supplemental Fig. 2). This may be due to the relatively high expression of both PGP1 and PGP19 in root apices and correlates well with the proposed role of these proteins in establishing directional auxin movement away from apical tissues (4). However, in addition to reduced peak area, IAA influxes in both *twd1* and *pgp1*/*pgp19* roots were localized more apically (0.05–0.35 mm) compared with the wild-type roots (0.1–0.45 mm) and *pgp1* and *pgp19* single mutant roots (0.1–0.35 mm). Apical shifts have been reported for maize *semaphore* and *lrt1 rum1* mutants, which are also defective in auxin transport (49). A recent report employing microelectrodes showed that the transition zone presents peaks in

the fluxes of O_2, K^+, and H^+ (48), which make this region the most active region of the root. As a consequence, a shift in this active region of 0.5–1 mm could affect many aspects of root physiology and development.

It has been suggested that some mammalian and plant FKBPs possess chaperone activity and play a role in protein secretion (36). To investigate if loss of *TWD1* function does alter the targeting of auxin efflux complexes, PIN1 and PIN2 were immunolocalized in wild-type and *twd1* root tips. PIN1 and PIN2 have been shown to play essential roles as components of the auxin efflux complex, are expressed in the same tissues as PGP1, and are co-purified with PGP1 and PGP19 by NPA affinity chromatography (4, 10, 17). Neither PIN1 nor PIN2 was mislocalized in *twd1* (Fig. 2*A*), suggesting that altered PIN localization is not responsible for the reduced IAA export in *twd1*. The same was found when PIN1 and PIN2 were immunolocalized in sucrose gradient fractions from wild-type, *pgp1*/*pgp19*, and *twd1* plants (data not shown). Furthermore, PIN1 and PIN2 expression has been shown recently not to be altered in *pgp1* and *pgp19* roots (17).

To investigate *PGP1* expression and location in the *twd1* background, we analyzed the expression of a Pro_{PGP1}-PGP1-c-Myc construct (17) in *twd1* mutants. PGP1 was co-localized with H^+-ATPase using anti-c-Myc antibody in plasma membrane fractions obtained by continuous sucrose gradient fractionation and showed no significant difference in expression compared with the wild type (Fig. 2*B*). Similar results were obtained using *twd1* membrane fractions and an antiserum recognizing both PGP1 and PGP19 (supplemental Fig. 5). Furthermore, *PGP1* transcript levels were unaltered in both *twd1* and TWD1-overexpressor as measured by RT-PCR (Fig. 2*C*). The unaltered expression levels and localization of auxin efflux proteins in *twd1* mutants indicate that TWD1 may function not by altering the localization of PGPs, but instead by regulating the function of PGPs via protein-protein interactions.

PGP19 Mediates Auxin Export When Expressed in HeLa Cells—Cellular IAA efflux experiments using plant protoplasts suggested that PGP19 might function in auxin export in a manner similar to PGP1 (17). In contrast to PGP1, however, PGP19-mediated auxin transport could not be tested in transgenic yeast, as PGP19 was shown to be improperly localized upon expression in yeast, most likely because of hyperglycosylation (15, 17). To demonstrate the role of PGP19 in auxin transport, we functionally expressed PGP19 in the vaccinia virus HeLa cell expression system, which has become a standard system for assaying mammalian PGP transport activity (37) and which we have used previously to demonstrate PGP1-mediated auxin efflux (17).

Heterologous expression of PGP19 in HeLa cells provided evidence that, similar to PGP1, PGP19 functions as an ATP-activated anion channel capable of mediating auxin efflux. Expression of PGP19 in HeLa cells resulted in net efflux of IAA over a 6-fold concentration range (10–63 nM) (Fig. 3*A* and supplemental Fig. 4) and a lower but significant export of 1-naphthylacetic acid (NAA). The antiauxin 2-NAA was not exported (Fig. 3*B*). As was shown for PGP1 (17), PGP19 did not exhibit the broad substrate specificity common to mammalian PGP transporters and failed to transport standard MDR substrates,

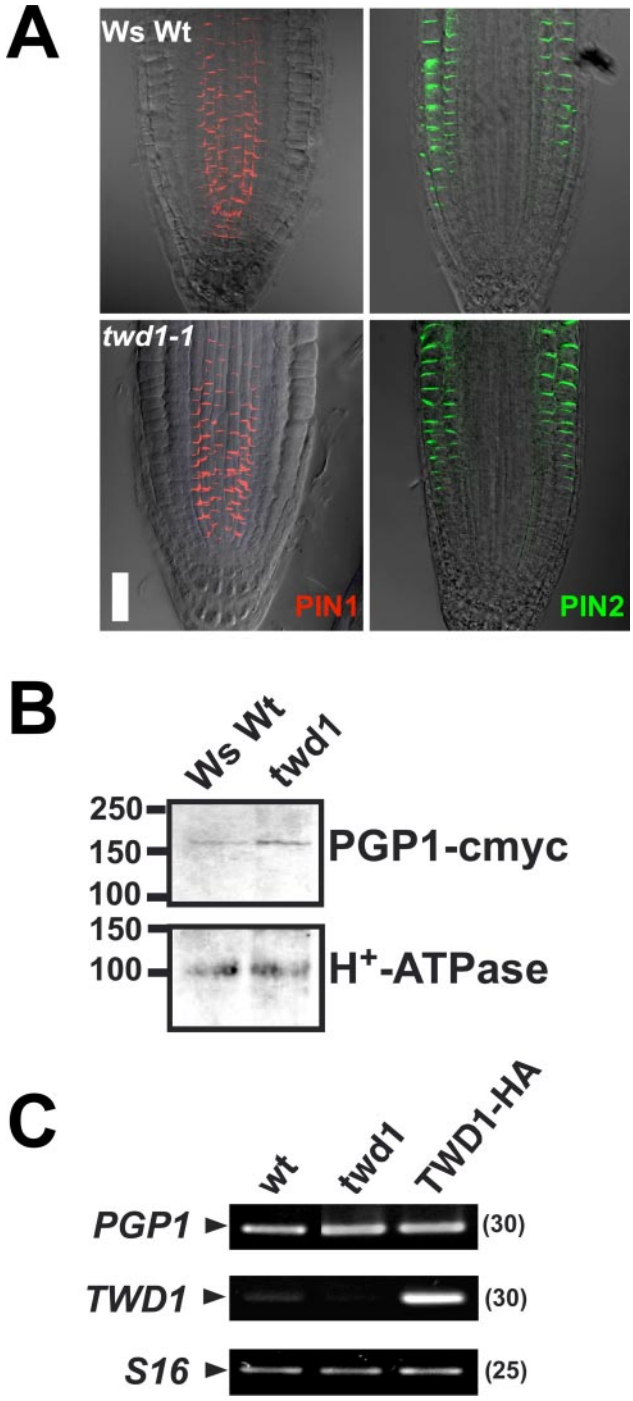

FIGURE 2. **Loss of function of TWD1 does not alter expression and localization of components of the auxin efflux complex such as PIN1, PIN2, and PGP1.** *A*, whole mount immunolocalization of auxin facilitator proteins PIN1 (*red*) and PIN2 (*green*), components of the auxin efflux complex, revealed no significant changes in expression. For orientation, colored fluorescence images were superimposed with bright-field pictures. *Scale bar* = 100 μm. *Ws Wt*, wild-type ecotype Wassilewskija. *B*, shown are the results from Western analysis of Pro_{PGP1}-PGP1-c-Myc in wild-type and *twd1* plasma membrane-enriched fractions as verified by immunodetection of the plasma membrane marker H^+-ATPase. *C*, loss and gain of function of *TWD1* had no significant effect on PGP1 expression as shown by semiquantitative RT-PCR.

including rhodamine 123, daunomycin, and BODIPY-vinblastine in fluorescence-activated cell sorter assays (supplemental Fig. 3) (17). Similar to PGP1, PGP19 mediated efflux of benzoic acid only at higher concentrations (63 nM), but not at lower

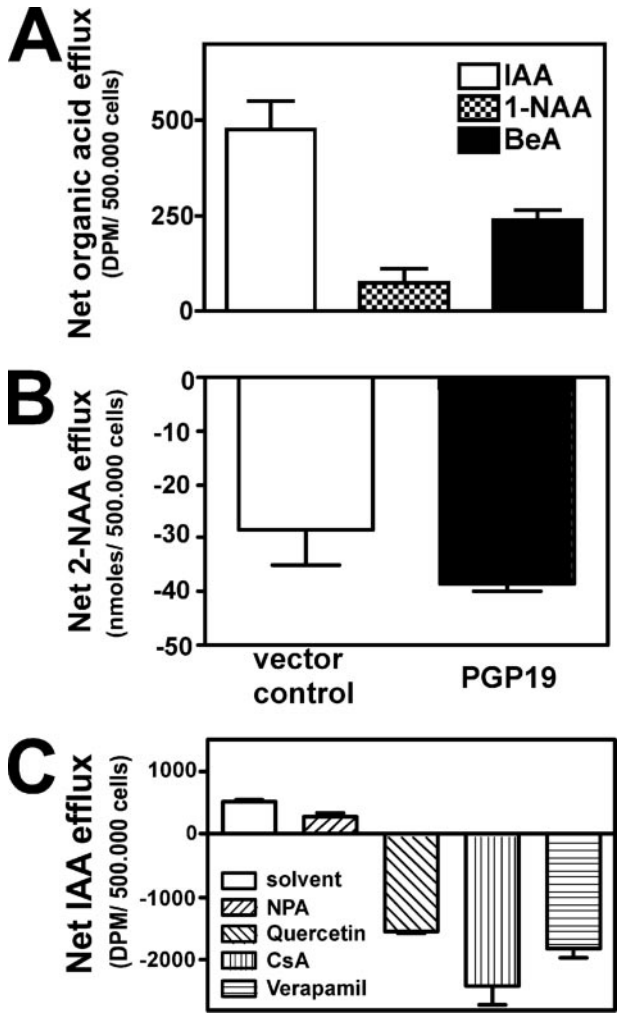

FIGURE 3. **PGP19 mediates auxin export when expressed in HeLa cells.** *A*, [^{3}H]IAA efflux was increased in HeLa cells expressing *PGP19*. PGP1 also modulated efflux of 1-[^{3}H]NAA and [^{3}H]benzoic acid (*BeA*). *B*, 2-NAA was retained in HeLa cells expressing *PGP19*. Cells were incubated with 62.59 nM unlabeled 2-NAA. 2-NAA levels were measured by liquid chromatography-mass spectrometry. Data are presented as nanomoles of 2-NAA/500,000 cells (means ± S.D.) and represent values obtained from two experiments with three replicates each. *C*, [^{3}H]IAA efflux by PGP19 was inhibited by treatment with 10 μM NPA, 200 nM quercetin, and the ABC transport inhibitors cyclosporin A (*CsA*) and verapamil when cells were loaded with 10 nM radiolabeled substrate. Net efflux (the amount of auxin retained by cells transformed with empty vector minus the amount of auxin retained by cells transformed with PGP19) is expressed as disintegrations/min/500,000 cells. Reductions in auxin retention (efflux) in transformed cells are presented as positive values. In all cases, expression and localization of *PGP19* were confirmed by RT-PCR (55) and Western blotting (37) using standard protocols for the system. Cell viability after treatment was confirmed visually and via cell counting. Data are the means ± S.D. ($n = 3$).

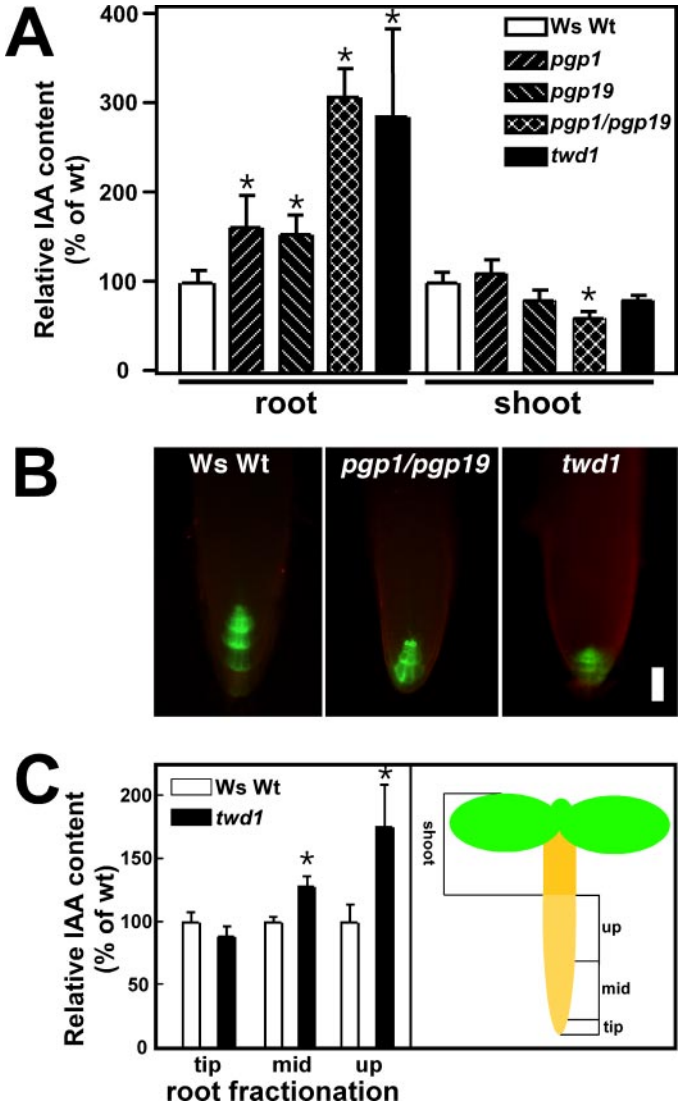

FIGURE 4. **IAA content in *twd1* and *pgp1*/*pgp19* roots is elevated.** *A*, relative free IAA content compared with the wild type in 9-day seedlings was determined by GC-MS. Absolute wild-type values were 42.2 ± 5.7 and 49.9 ± 6.1 pg/mg (fresh weight) for roots and shoots, respectively. *Ws Wt*, wild-type ecotype Wassilewskija. *, significantly different from the wild type ($p < 0.05$, analysis of variance). *B*, Pro$_{DR5}$-GFP expression in 9-day seedling root tips showed no significant differences compared with the wild type. *C*, fractionation of 9-day seedling roots indicated elevated free IAA levels in the root elongation zone and above. *cot*, cotyledon; *hyp*, hypocotyl. *, significantly different from the wild type ($p < 0.05$, analysis of variance).

concentrations (10 nM), at which auxin efflux activities were still active (supplemental Fig. 4) (17). Finally, PGP19 expression also increased the efflux of oxidative IAA breakdown products in a manner similar to PGP1 expression (supplemental Fig. 4) (17).

Arabidopsis PGPs have been shown to bind the auxin transport inhibitors quercetin (an aglycone flavonoid) and NPA (16, 22). PGP19-mediated IAA efflux from HeLa cells was inhibited by both NPA and quercetin as well as by the mammalian PGP inhibitors cyclosporin A and vinblastine (Fig. 2*C*).

Roots of twd1 and pgp1/pgp19 Reveal Greatly Elevated Free Auxin Levels and Altered Gravitropism—Previously, both reduced basipetal auxin transport and reduced IAA levels were reported in 5-day post-germination *pgp1* and *pgp19* mutant roots (17). We analyzed free IAA levels in root and shoot tissues (see Fig. 4*C* for the experimental setup) of 9-day post-germination *twd1* and *pgp* mutant seedlings. Absolute values for wild-type tissues were slightly higher but in the same range as reported by others (68). Surprisingly and in contrast to 5-day roots, we found elevated IAA levels in all mutant roots, whereas the levels in mutant shoots revealed only small differences compared with wild-type levels (Fig. 4*A*). Interestingly, the IAA content in *pgp1*/*pgp19* (308%) and *twd1* (286%) roots was clearly higher than that in *pgp1* (162%) and *pgp19* (154%) roots.

This again suggests functional redundancy of PGP1 and PGP19 and a loss of function of PGP1/PGP19-mediated IAA auxin transport in *twd1*.

To investigate alterations in local auxin concentrations in more detail, we analyzed expression of the auxin reporter construct Pro_{DR5}-GFP (38) in *twd1* and *pgp* mutant root tips. This method was selected as it allows a more noninvasive detection of IAA concentrations compared with the more commonly used Pro_{DR5}-β-glucuronidase construct. 9-Day *pgp1*/*pgp19* and *twd1* roots showed slightly reduced reporter gene expression in root columella cells compared with wild-type roots (Fig. 4*B*). Consistent with previously published Pro_{DR5}-β-glucuronidase data from 5-day post-germination seedlings (17, 18), similar results were observed in *pgp1* and *pgp2* single mutants (data not shown).

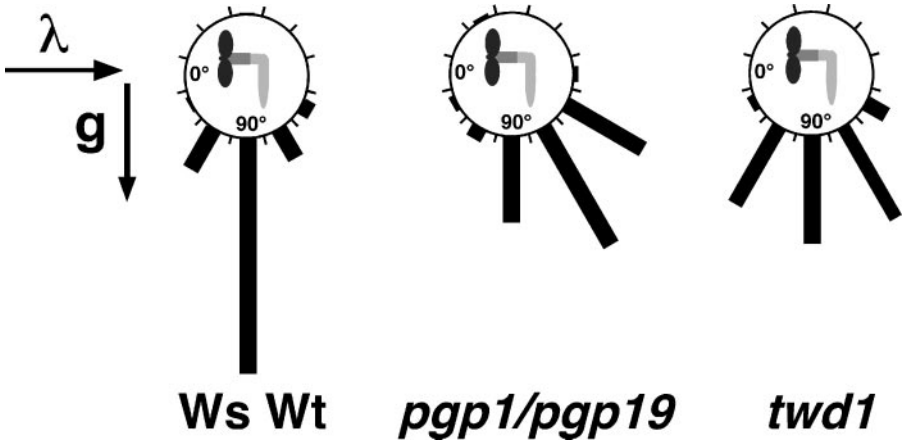

FIGURE 5. ***twd1* and *pgp1*/*pgp19* seedlings are defective in root gravitropism.** For quantification of gravitropism, plants were grown on vertical plates under continuous light conditions (coming from the left as indicated by the *arrow*) (61). Each gravistimulated root was assigned to one of twelve 30° sectors in the circular histograms; the length of each *bar* represents the percentage of seedlings showing the same direction of root growth. The number of seedlings for each genotype was between 72 and 96. *Ws Wt*, wild-type ecotype Wassilewskija.

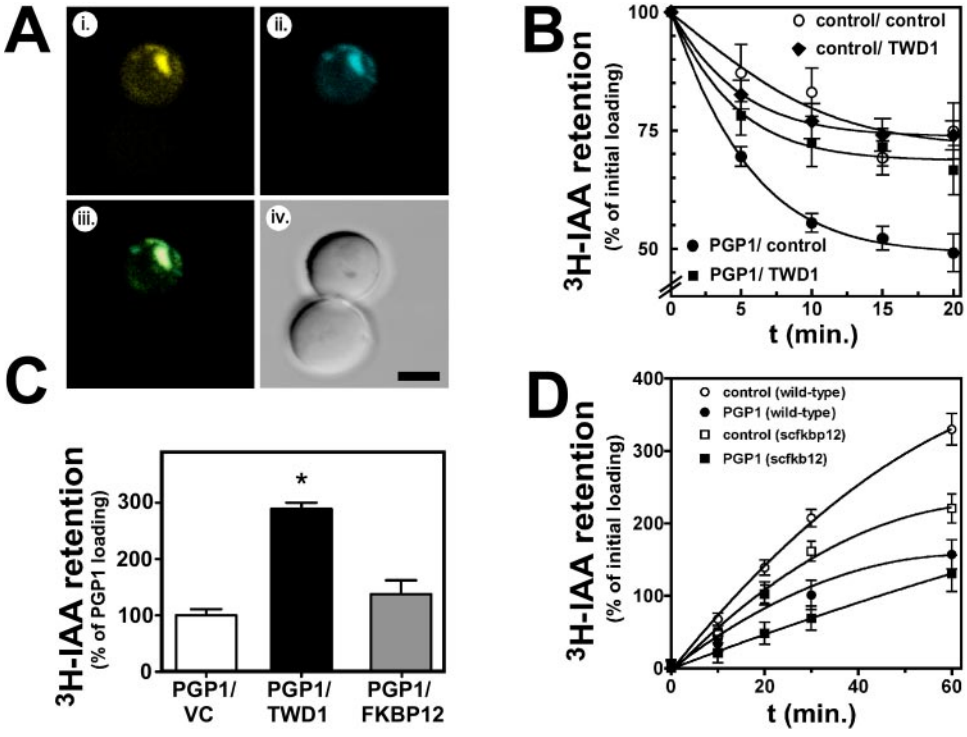

FIGURE 6. **Coexpression of PGP1 and TWD1 specifically inhibits IAA export.** *A*, PGP1-YFP (*upper left panel*) was expressed on the plasma membrane and in raft-like structures and co-localized with TWD1-CFP (*lower left panel*) in yeast as shown by superimposition (*upper right panel*). Differential interference contrast images of the same cells are shown (*lower right panel*). *Scale bar* = 2.5 μm. *B*, coexpression of TWD1 and PGP1 reduced PGP1-mediated IAA export to vector control levels. Reductions in auxin retention (efflux) are presented as relative export of the initial loading. Data are the means ± S.D. ($n = 4$). *C*, coexpressed *Arabidopsis* FKBP12 did not significantly alter PGP1-mediated IAA efflux. Reductions in auxin retention (efflux) after 10 min are presented as relative export of the initial loading. Data are the means ± S.D. ($n = 3$). *, significantly different from the PGP1/vector control (*VC*; $p < 0.05$, analysis of variance test). *D*, PGP1-mediated IAA efflux was not dependent on *S. cerevisiae* (*Sc*) FKBP12/FPR as shown by assaying IAA efflux in an *fpr1* strain and the corresponding wild-type strain. Reductions in auxin retention (efflux) are presented as relative loading of the initial loading. Data are the means ± S.D. ($n = 3$).

Reduction of auxin levels visualized by the reporter gene constructs seemed to contradict at first glance the elevated IAA concentrations measured by GC-MS. Therefore, we dissected *twd1* roots into three parts (Fig. 4*C*) and determined the free IAA concentrations of each segment. GC-MS analysis revealed that auxin levels in the "tip" (the region 2 mm from the tip) were indeed slightly reduced (89% of the wild-type levels), whereas the mid-part (128%) and upper part (176%) root fractions contained significantly higher levels (Fig. 4*C*). The total IAA levels in this assay were lower than those observed in GC-MS analysis of whole root tissues, possibly because of the unavoidable drastic manipulation during fractionation.

Root gravitropism is known to be dependent on and to be mediated by polar auxin transport (59). Therefore, gravitropic growth tests are an ideal tool to investigate the developmental effects of the alterations in auxin fluxes observed in *twd1* and *pgp* mutants. Previous studies have demonstrated that *pgp19* and *pgp1*/*pgp19* hypocotyls exhibit enhanced gravitropic responses (39). Under standard gravitropism assay conditions, the roots of *pgp1* and *pgp19* single mutants exhibited no significant changes in gravitropism (data not shown). However, both *pgp1*/*pgp19* and *twd1* exhibited impaired gravitropic responses compared with the wild type (Fig. 5).

Consistent with previous results in hypocotyl tissues (39), *pgp1*/*pgp19* roots exhibited slight hypergravitropism, whereas *twd1* roots showed impaired gravitropism without any directional preference.

Modulation of PGP1-mediated IAA Export by TWD1 Is Specific and Has Reverse Effects in Yeast and Mammalian Cells—To investigate the regulatory effect of TWD1 on PGP activity in more detail, we coexpressed PGP1 and TWD1 in the yeast *S. cerevisiae*. In yeast, PGP1 and TWD1 co-localized mainly with some unknown punctate structures in the vicinity of the plasma membrane as demonstrated by confocal microscope analysis of PGP1-YFP and TWD1-CFP (Fig. 6*A*) and Western detection of plasma membrane-enriched fractions of yeast membranes coexpressing TWD1 and PGP1 (data not shown). Furthermore, coexpression of PGP1-YFP and TWD1 N-terminally fused to *Renilla* luciferase in yeast resulted in a positive bioluminescence resonance energy transfer ratio, verifying the interaction.[4]

Monitoring time-dependent PGP1-mediated IAA efflux (measured as decreased IAA retention) in yeast revealed that coexpression reverted export toward the vector control level (Fig. 6*B*), whereas TWD1 alone had only a slight inhibitory effect on background IAA efflux. The same tendency was found when loading kinetics were recorded (see "Experimental procedures") (supplemental Fig. 6). Similarly, TWD1 inhibited PGP1-mediated detoxification of the toxic auxin analog 5-fluoroindole (supplemental Fig. 6*C*), which has been used to demonstrate PIN2/AGR1 function in yeast (41).

Inhibition of PGP1-mediated IAA efflux in yeast by TWD1 was specific, as expression of TWD1 alone had no significant effect on background IAA efflux (Fig. 6*B*). Furthermore, *Arabidopsis* FKBP12, which represents the most basic FKBP, consisting essentially just of the *cis*,*trans*-peptidylprolyl isomerase domain, and which functions as a cell cycle regulator (42), reduced PGP1-mediated IAA efflux (measured as increased IAA retention) only slightly compared with TWD1 (Fig. 6*C*). In the *yap1-1* mutant, only TWD1 (but not the closely related *Arabidopsis* proteins FKBP12 and ROF1/FKBP59) (62), significantly inhibited PGP1-mediated IAA detoxification (supplemental Fig. 6*B*). Finally, yeast FKBP12 seemed to somehow activate PGP1-mediated IAA export, resulting in reduced IAA loading in the *S. cerevisiae* FKBP12 mutant (Fig. 6*D*), which confirms previous results on murine MDR3 activity (33). However, the same magnitude of stimulation was found also for the background activity (Fig. 6*D*, vector control), suggesting unspecific up-regulation of yeast endogenous export systems.

Inhibition of PGP1 by TWD1 in yeast was surprising, as an opposite effect was expected based on the protoplast efflux assays described above. Therefore, we coexpressed PGP1 and TWD1 in HeLa cells, which represent the standard expression system for analyzing mammalian ABCs (37). Interestingly, TWD1 conferred stimulation of PGP1-mediated auxin efflux upon coexpression (Fig. 7). The influence of TWD1 on PGP19 could be tested in neither yeast nor HeLa cells, as PGP19 is inactive in yeast (15, 17), whereas coexpression of PGP19 and TWD1 had destabilizing effects on the HeLa cells (data not shown).

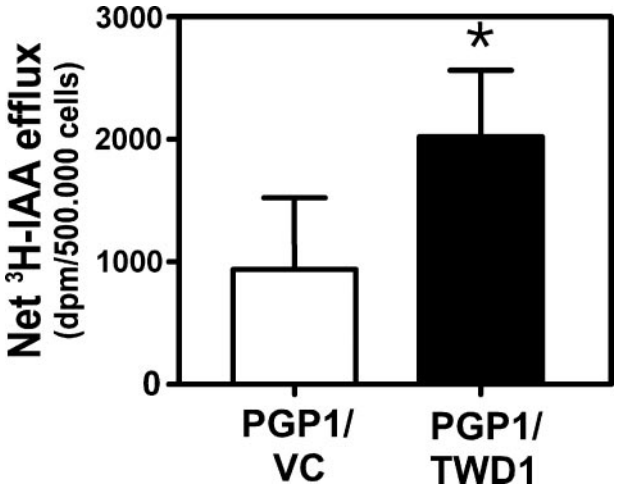

FIGURE 7. **Coexpression of PGP1 and TWD1 enhances PGP1-mediated IAA export in HeLa cells.** Shown is the efflux of radiolabeled IAA from HeLa cells expressing PGP1 with the indicated ratios of TWD1. Reduction in auxin retention (efflux) is presented as net efflux. Expression and localization of expressed proteins were confirmed by RT-PCR and Western analysis (data not shown). Data are the means ± S.D. ($n = 3$). *, significantly different from the PGP1/vector control (*VC*; $p < 0.05$, analysis of variance).

DISCUSSION

To understand the strong developmental phenotype that is caused by loss of function of *Arabidopsis* TWD1/FKBP42, we previously demonstrated interactions between TWD1 and the MDR/PGP transporters PGP1 and PGP19 (16). As both PGP1 and PGP19 have been shown to be capable of catalyzing export of the critical plant hormone auxin (17), a regulatory role of TWD1 in PGP1/PGP19 has been suggested to account for the auxin-related aspects of the *twd1* phenotype. An emerging function of immunophilins is their role in regulating large membrane proteins such as rhodopsin (43) or integral Ca^{2+} channels such as the ryanodine and 1,4,5-triphosphate receptors (31, 44). Regulation of murine MDR3 by yeast FKBP12 has also been demonstrated, although the effects of mammalian PGP-FKBP interactions *in vivo* have not yet been fully investigated (33).

In this study, we have provided several lines of evidence that TWD1 is an essential regulatory component of the PGP-mediated auxin efflux complex *in planta* by means of protein-protein interactions. PGP1-TWD1 and PGP19-TWD1 interactions have been previously demonstrated by yeast two-hybrid analysis, NPA affinity chromatography, and co-immunoprecipitation pulldown assays (4, 16, 22).

1) Cellular efflux of IAA from mutant cells is reduced compared with that from wild-type cells in the order wild type > *pgp1* > *pgp19* ≫ *pgp1*/*pgp19* ≥ *twd1*. The magnitude of reduction correlates with both whole plant transport data (16) and with the observable auxin-deficient mutant phenotypes (16, 17). Overexpression of TWD1 has no effect on IAA export, whereas up-regulation of the ABC transporters PGP1 and PGP19 strongly enhances efflux.

2) Expression and localization of PIN1 and PIN2 (essential components of the auxin efflux complex) are not altered in

[4] A. Bailly and M. Geisler, unpublished data.

twd1. Based on RT-PCR and Western analysis, the same seems to be true for PGP1. The observed reduction of auxin export is therefore unlikely due to altered expression or mistargeting of PGPs and PIN proteins. Activation of the transport complex through TWD1 must therefore rely on the physical interaction of TWD1 with the remainder of the transport complex.

3) Modulation by TWD1 is gene-specific, as the related *Arabidopsis* proteins FKBP12 (28, 42) and ROF1/FKBP59 (62) have only slight effects on PGP1-mediated IAA transport compared with TWD1 when coexpressed with PGP1 in yeast. Surprisingly, coexpression of TWD1 in yeast *versus* protoplast and mammalian cells showed opposite effects on PGP1 activity (inhibition in yeast and stimulation in HeLa cells), suggesting that plant-specific components might be absent in the unicellular eukaryote *S. cerevisiae*. Currently, we are trying to identify the factors that modulate the activity of TWD1 in these systems. Reversible protein phosphorylation by protein kinases might be a possible mechanism, as mammalian PGPs are known to be regulated via phosphorylation (45, 46). Interestingly, PGP1 has been recently shown to be phosphorylated in a so-called regulatory linker domain (47). Another intriguing possibility is that FKBP-interacting proteins (50) might be lacking in yeast. Interestingly, many effects of immunosuppressant drugs are not seen in yeast.

In our current model of a PGP1-TWD1-PGP19 auxin efflux complex, functional interactions take place between the C-terminal nucleotide-binding fold (NBF2) of PGP1 and the N-terminal *cis*,*trans*-peptidylprolyl isomerase-like domain of TWD1, whereas PGP19 apparently requires the full TWD1 protein (16). The nucleotide-binding folds of the PGPs do not interact with each other,[5] which is of interest, as mammalian ABC transporters have been suggested to function as heterodimers (57). Therefore, we postulate that TWD1 functions as a linker between both PGPs, although the existence of the ternary complex awaits confirmation.

The simplest mechanistic model based on our data would have TWD1-induced conformational changes in the C termini of PGP1 and PGP19 increase ATP access to the second ATP-binding sites of these proteins (NBF2). In the absence of TWD1, the ATP-binding sites would be blocked, leaving PGP1/PGP19 in an inactive state. The activity of heterologously expressed PGP1 argues for activation by host endogenous factors that partially can take over TWD1 function. However, at this time, we cannot exclude that the regulatory domain shift effects alternatively or additionally substrate (IAA) binding. Recognition and binding of the great diversity of drugs by PGPs are still not fully understood (46).

Furthermore, the fact that overexpression of PGP1 and PGP19 results in increased IAA efflux argues either that TWD1 is not yet saturated by PGP1/PGP19 or that activation is a transient event. This has been suggested for the missing demonstration of a murine MDR3-FKBP12 complex in yeast (33). However, overexpression of TWD1 has no significant effect on IAA efflux that might favor a transient interaction.

In addition to this novel role for FKBPs, we have also demonstrated a direct involvement of TWD1 in auxin transport that is at least partially able to explain the drastic overlapping developmental phenotype of both *twd1* and *pgp1*/*pgp19* plants. Loss of function of PGP1/PGP19-mediated auxin export in *twd1* blocks basipetal polar auxin transport (shown for *pgp1* and *pgp19*) (17), resulting in elevated free IAA levels in mature root parts. This correlates with polar (dominantly basal) expression of PGP1 in the mature root regions (17). Alternatively, non-polar expression of PGP1 in meristematic cells of the root apex (17) has been suggested to function as a sink in long-range transport of IAA (13). This further verifies an involvement of PGP1/PGP19 and TWD1 in long-distance transport of IAA, as has been suggested previously (17, 18).

Agravitropic roots and many aspects of the strong developmental phenotype of *twd1* and *pgp1*/*pgp19* plants are in good agreement with altered polar auxin transport and elevated auxin concentrations in the roots. Other growth defects especially in the shoots might be a consequence of altered reflux of auxin into the shoots or of secondary effects. Reduced and apically shifted influx maxima that have been verified for *pgp* and *twd1* roots using an auxin-specific electrode in analogy to other auxin transport mutants (49) suggest indeed altered reflux capacities.

However, the "twisted syndrome" not seen in *pgp1*/*pgp19* plants suggests that other TWD1-specific functions are missing in *twd1*. In this respect, it is important to keep in mind that the multidomain FKBP TWD1 interacts additionally with HSP90, calmodulin, and MRP-like ABC transporters MRP1 and MRP2 (16, 29, 30), which might account for the more severe phenotype by loss of additional functions.

The precise expression pattern of TWD1 and PGP19 is still not known, and co-immunolocalization of all components has failed so far because of the extremely low abundance of TWD1 (16). Attempts to localize TWD1 in wild-type cells using antisera or CFP fusions have failed so far.[6] The low expression of TWD1 compared with that of the PGPs as shown by RT-PCR and *in silico* data (www.genevestigator.ethz.ch) (data not shown) further supports a transient but highly functional interaction of TWD1 and PGPs. However, careful gene chip analysis revealed that *TWD1*, despite its low abundance, is coexpressed in virtually all tissues with *PGP1*/*PGP19* and that the expression of all three genes is induced by various common stresses (data not shown).

Finally, our experimental evidence provided here suggests that this mode of PGP regulation by protein-protein interaction might be relevant beyond plants. Transfer of this novel FKBP function could be beneficial for development of novel strategies for cancer therapy via FKBP-mediated down-regulation of drug efflux.

Acknowledgments—We are grateful to Drs. P. Lariguet and C. Fankhauser for help during gravity assays, Drs. A. Düchtig and A. Müller for analyzing free IAA contents, Drs. J. Heitman and G. R. Fink for mutant yeast strains, and Dr. E. Martinoia for continuous support.

REFERENCES

1. Benkova, E., Michniewicz, M., Sauer, M., Teichmann, T., Seifertova, D., Jürgens, G., and Friml, J. (2003) *Cell* **115,** 591–602

[5] R. Bouchard and M. Geisler, unpublished data.

[6] B. Schulz and M. Geisler, unpublished data.

2. Friml, J., and Wisnieswska, J. (2005) *Intercellular Communication in Plants* (Fleming, A., ed) pp. 1–26, Blackwell Publishing, Oxford
3. Baluska, F., Samaj, J., and Menzel, D. (2003) *Trends Cell Biol.* **13,** 282–285
4. Blakeslee, J. J., Peer, W. A., and Murphy, A. S. (2005) *Curr. Opin. Plant Biol.* **8,** 1–7
5. Blilou, I., Xu, J., Wildwater, M., Willemsen, V., Paponov, I., Friml, J., Heidstra, R., Aida, M., Palme, K., and Scheres, B. (2005) *Nature* **433,** 39–44
6. Friml, J. (2003) *Curr. Opin. Plant Biol.* **6,** 7–12
7. Folkes, K. L., and Wardman, P. (2003) *Cancer Res.* **63,** 776–779
8. Goldsmith, M. H. M. (1977) *Annu. Rev. Plant Physiol.* **28,** 439–478
9. Lomax, T. L., Mehlhorn, R. J., and Briggs, W. R. (1995) *Proc. Natl. Acad. Sci. U. S. A.* **82,** 6541–6545
10. Petrášek, J., Mravec, J., Bouchard, R., Blakeslee, J. J., Abas, M., Seifertová, D., Wiśniewska, J., Tadele, J., Čovanová, M., Dhonukshe, P., Skůpa, P., Benková, E., Perry, L., Křeček, P., Lee, O. R., Fink, G. R., Geisler, M., Murphy, A. S., Luschnig, C., Zažímalová, E., and Friml, J. (2006) *Science* **12,** 914–918
11. Martinoia, E., Klein, M., Geisler, M., Bovet., L., Forestier, C., Kolukisaoglu, H. Ü., Müller-Röber, B., and Schulz, B. (2002) *Planta* **214,** 345–355
12. Jasinski, M., Ducos, E., Martinoia, E., and Boutry, M. (2003) *Plant Physiol.* **131,** 1169–1177
13. Geisler, M., and Murphy, A. S. (2006) *FEBS Lett.* **580,** 1094–1102
14. Krishna, R., and Mayer, L. D. (2001) *Curr. Med. Chem. Anticancer Agents* **1,** 163–174
15. Noh, B., Murphy, A. S., and Spalding, E. P. (2001) *Plant Cell* **13,** 2441–2454
16. Geisler, M., Kolukisaoglu, H. Ü., Bouchard, R., Billion, K., Berger, J., Saal, B., Frangne, N., Koncz-Kalman, Z., Koncz, C., Dudler, R., Blakeslee, J. J., Murphy, A. S., Martinoia, E., and Schulz, B. (2003) *Mol. Biol. Cell* **14,** 4238–4249
17. Geisler, M., Blakeslee, J. J., Bouchard, R., Lee, O. R., Vincenzetti, V., Bandyopadhyay, A., Titapiwatanakun, B., Peer, W. A., Bailly, A., Richards, E. L., Ejendal, K. F., Smith, A. P., Baroux, C., Grossniklaus, U., Müller, A., Hrycyna, C. A., Dudler, R., Murphy, A. S., and Martinoia, E. (2005) *Plant J.* **44,** 179–196
18. Lin, R., and Wang, H. (2005) *Plant Physiol.* **138,** 949–964
19. Multani, D. S., Briggs, S. P., Chamberlin, M. A., Blakeslee, J. J., Murphy, A. S., and Johal, G. S. (2003) *Science* **302,** 81–84
20. Santelia, D., Vincenzetti, V., Bovet, L., Fukao, Y., Düchtig, P., Martinoia, E., and Geisler, M. (2005) *FEBS Lett.* **579,** 5399–5406
21. Terasaka, K., Blakeslee, J. J., Titapiwatanakun, B., Peer, W. A., Bandyopadhyay, A., Makam, S. N., Lee, O. R., Richards, E., Murphy, A. S., Sato, F., and Yazaki, K. (2005) *Plant Cell* **17,** 2922–2939
22. Murphy, A. S., Hoogner, K. R., Peer, W. A., and Taiz, L. (2002) *Plant Physiol.* **128,** 935–950
23. Perez-Perez, J. M., Ponce, M. R., and Micol, J. L. (2004) *Plant Physiol.* **134,** 101–117
24. Romano, P., Gray, J., Horton, P., and Luan, S. (2005) *New Phytol.* **166,** 753–769
25. Faure, J. D., Vittorioso, P., Santoni, V., Fraisier, V., Prinsen, E., Barlier, I., Van Onckelen, H., Caboche, M., and Bellini, C. (1998) *Development* (*Camb.*) **125,** 909–918
26. Vittorioso, P., Cowling, R., Faure, J. D., Caboche, M., and Bellini, C. (1998) *Mol. Cell. Biol.* **18,** 3034–3043
27. Kurek, I., Pirkl, F., Fischer, E., Buchner, J., and Breiman, A. (2002) *Planta* **215,** 119–126
28. Harrar, Y., Bellini, C., and Faure, J. D. (2001) *Trends Plant Sci.* **6,** 426–431
29. Kamphausen, T., Fanghänel, J., Neumann, D., Schulz, B., and Rahfeld, J.-U. (2002) *Plant J.* **32,** 263–276
30. Geisler, M., Girin, M., Brandt, D., Vincenzetti, V., Plaza, S., Paris, N., Kobae, Y., Maeshima, M., Billion, K., Kolukisaoglu, H. Ü., Schulz, B., and Martinoia, E. (2004) *Mol. Biol. Cell* **15,** 3393–3405
31. Cameron, A. M., Steiner, J. P., Roskams, A. J., Ali, S. M., Ronnett, G. V., and Snyder, S. H. (1995) *Cell* **83,** 463–472
32. Peer, W. A., Bandyopadhyay, A., Blakeslee, J. J., Makam, S. N., Chen, R. J., Masson, P. H., and Murphy, A. S. (2004) *Plant Cell* **16,** 1898–1911
33. Hemenway, C. S., and Heitman, J. (1996) *J. Biol. Chem.* **271,** 18527–18534
34. Mealey, K. L., Barhoumi, R., Burghardt, R. C., McIntyre, B. S., Sylvester, P. W., Hosick, H. L., and Kochevar, D. T. (1999) *Cancer Chemother. Pharmacol.* **44,** 152–158
35. Mancuso, S., Marras, A. M., Magnus, V., and Baluska, F. (2005) *Anal. Biochem.* **341,** 344–351
36. Schiene, C., and Fischer, G. (2000) *Curr. Opin. Struct. Biol.* **10,** 40–45
37. Hrycyna, C. A., Ramachandra, M., Pastan, I., and Gottesman, M. M. (1998) *Methods Enzymol.* **292,** 456–473
38. Ottenschläger, I., Wolff, P., Wolverton, C., Bhalerao, R. P., Sandberg, G., Ishikawa, H., Evans, M., and Palme, K. (2003) *Proc. Natl. Acad. Sci. U. S. A.* **100,** 2987–2991
39. Noh, B., Bandyopadhyay, A., Peer, W. A., Spalding, E. P., and Murphy, A. S. (2003) *Nature* **423,** 999–1002
40. Prusty, R., Grisafi, P., and Fink, G. R. (2004) *Proc. Natl. Acad. Sci. U. S. A.* **101,** 4153–4157
41. Luschnig, C., Gaxiola, R. A., Grisafi, P., and Fink, G. R. (1998) *Genes Dev.* **12,** 2175–2187
42. Aghdasi, B., Ye, K., Resnick, A., Huang, A., Ha, H. C., Guo, X., Dawson, T. M., Dawson, V. L., and Snyder, S. H. (2001) *Proc. Natl. Acad. Sci. U. S. A.* **98,** 2425–2430
43. Stamnes, M. A., Shieh, B. H., Chuman, L., Harris, G. L., and Zuker, C. S. (1991) *Cell* **65,** 219–227
44. Timerman, A. P., Wiederrecht, G., Marcy, A., and Fleischer, S. (1995) *J. Biol. Chem.* **270,** 2451–2459
45. Castro, A. F., Horton, J. K., Vanoye, C. G., and Altenberg, G. A. (1999) *Biochem. Pharmacol.* **58,** 1723–1733
46. Ambudkar, S. V., Kimchi-Sarfaty, C., Sauna, Z. E., and Gottesman, M. M. (2003) *Oncogene* **22,** 7468–7485
47. Nühse, T. S., Stensballe, A., Jensen, O. N., and Peck, S. C. (2004) *Plant Cell* **16,** 2394–2405
48. Mancuso, S., and Marras, A. M. (2006) *Plant Cell Physiol.* **47,** 401–409
49. Schlicht, M., Strnad, M., Scanlon, M. J., Mancuso, S., Hochholdinger, F., Palme, K., Volkmann, D., Menzel, D., and Baluška, F. (2006) *Plant Signal. Behav.* **1,** 134–139
50. Vespa, L., Vachon, G., Berger, F., Perazza, D., Faure, J. D., and Herzog, M. (2004) *Plant Physiol.* **134,** 1283–1292
51. Geisler, M., Frangne, N., Gomes, E., Martinoia, E., and Palmgren, G. M. (2000) *Plant Physiol.* **124,** 1814–1827
52. Dünnwald, M., Varshavsky, A., and Johnsson, N. (1999) *Mol. Cell. Biol.* **10,** 329–344
53. Arndt, C., Cruz, M. C., Cardenas, M. E., and Heitman, J. (1999) *Microbiology* **145,** 1989–2000
54. Cruz, M. C., Cavallo, L. M., Gorlach, J. M., Cox, G., Perfect, J. R., Cardenas, M. E., and Heitman, J. (1999) *Mol. Cell. Biol.* **19,** 4101–4112
55. Blakeslee, J. J., Bandyopadhyay, A., Peer, W. A., Makam, S. N., and Murphy, A. S. (2004) *Plant Physiol.* **134,** 28–31
56. Li, J., Yang, H., Peer, W. A., Richter, G., Blakeslee, J., Bandyopadhyay, A., Titapiwantakun, B., Undurraga, S., Khodakovskaya, M., Richards, E. L., Krizek, B., Murphy, A. S., Gilroy, S., and Gaxiola, R. (2005) *Science* **310,** 121–125
57. Ramaen, O., Sizun, C., Pamlard, O., Jaquet, E., and Lallemand, J. Y. (2005) *Biochem. J.* **391,** 481–490
58. Sidler, M., Hassa, P., Hasan, S., Ringli, C., and Dudler, R. (1998) *Plant Cell* **10,** 1623–1636
59. Muday, G., and DeLong, A. (2001) *Trends Plant Sci.* **6,** 535–542
60. Ueda, M., Matsui, K., Ishiguro, S., Sano, R., Wada, T., Papanov, I., Palme, K., and Okada, K. (2004) *Development* (*Camb.*) **131,** 2101–2111
61. Lariguet, P., and Fankhauser, C. (2004) *Plant J.* **40,** 826–834
62. Vucich, V. A., and Gasser, C. S. (1996) *Mol. Gen. Genet.* **252,** 510–517
63. Weiergraber, O. H., Eckhoff, A., and Granzin, J. (2006) *FEBS Lett.* **580,** 251–255